Electronic Supplementary Material (ESI) for Energy & Environmental Science.

Compatibility issues between electrodes and electrolytes in solid-state batteries

Yaosen Tian,[†a,b] Tan Shi,[†a,b] William Davidson Richards,[c] Juchuan Li,[b] Jae Chul Kim,[b] Shou-Hang Bo[*b] and Gerbrand Ceder[*a,b,c]

[†]Co-authorship

[*] Corresponding author: sbo@lbl.gov; gceder@berkeley.edu

[a]Department of Materials Science and Engineering, University of California Berkeley, Berkeley, CA 94720, USA

[b]Materials Science Division, Lawrence Berkeley National Laboratory, Berkeley, CA 94720, USA

[c]Department of Materials Science and Engineering, Massachusetts Institute of Technology, Cambridge, MA 02139, USA

Supporting information

Table S1: DFT calculations for all possible products of the reaction between Na_xMO_2 (x = 0.5 or 1.0) and Na_3PX_4

	$NaCrO_2$	$NaMnO_2$	$NaFeO_2$	$NaCoO_2$	$NaNiO_2$
Na_3PS_4	Na_3PO_4, Na_3PS_4, $NaCrO_2$, Na_3PSO_3, Na_3PS_3O, $Na_3P(SO)_2$, $NaCrS_2$	Na_2SO_4, Na_3PO_4, Na_3PS_4, Na_3PSO_3, Na_3PS_3O, $NaMnS_2$, MnS, MnO, $NaMnO_2$, $Na_3P(SO)_2$, Na_2MnS_2, $Na_4Mn_3S_5$	Na_2SO_4, Na_3PO_4, Na_3PS_4, $NaFeO_2$, Na_3PSO_3, Na_3PS_3O, FeS_2, Fe_3O_4, $Na_3P(SO)_2$, $Na_3(FeS_2)_2$	Na_2SO_4, Co, Na_3PO_4, Na_3PS_4, $NaCoO_2$, Na_3CoO_3, Co_9S_8, $NaCoS_2$, Na_2S, Na_3PSO_3, Na_3PS_3O, $Na_3P(SO)_2$	Ni_3S_4, Ni_3S_2, Na_2SO_4, $Na_6S_2O_9$, Na_3PO_4, Ni, Na_3PS_4, Na_3PSO_3, Na_2S, NaS, NiO, Na_3PS_3O, Na_4NiO_3, $Na_3P(SO)_2$, $Na_2Ni_3S_4$
Na_3PSe_4	Na_3PSe_4, Cr_2O_3, Na_3PO_4, $Na_4P_2O_7$, Na_3PSeO_3, $NaCrO_2$, $NaCrSe_2$, Na_3PSe_3O, Na_2Se	Na_3PSe_4, Na_2MnSe_3, $NaMnO_2$, NaSe, Mn_3O_4, MnO, $NaMnPO_4$, Na_2Se, Na_3PO_4	Na_3PSe_4, $FeSe_2$, FeSe, Na_3PSe_3O, Na_3PO_4, $Na_4P_2O_7$, Fe_2O_3, $NaFeO_2$, Na_3PSeO_3, Fe_2P, FeP, Fe_3O_4, FeO, Na_2Se	Na_3PSe_4, Na_3PSe_3O, $CoSe_2$, $Na_4P_2O_7$, Co_9Se_8, $NaCoO_2$, $NaCo_7O_{11}$, Na_3PSeO_3, Co_2P, Co_3O_4, CoO, Co_5Se_8, Na_2Se, Na_3PO_4	Na_3PSe_4, Ni_2P, Ni_3Se_4, NiO, $Na_4P_2O_7$, $Ni_{12}P_5$, Na_5NiO_4, Na_3PSeO_3, Ni_5Se_8, Na_2SeO_3, $NiSe_2$, NaSe, Na_3PSe_3O, Na_2Se, Na_3PO_4

(Continued)

	$Na_{0.5}CrO_2$	$Na_{0.5}MnO_2$	$Na_{0.5}FeO_2$	$Na_{0.5}CoO_2$	$Na_{0.5}NiO_2$
Na_3PS_4	Na_2SO_4, Cr_2O_3, Na_3PO_4, $Na_6Cr(SO_4)_4$, Na_3PS_4, $Na_4P_2O_7$, $NaCrO_2$, $Na_3Cr(PO_4)_2$, Na_2PS_3, Na_3PSO_3, $Na_3P(SO)_2$, S, $Na_{2/3}CrS_2$, $Na_3Cr_2(PS_4)_3$, Na_3PS_3O, $NaCrS_2$	Na_2SO_4, $NaMnO_2$, $NaMnS_2$, Na_3PS_4, MnS, Mn_3S_4, Na_3PS_3O, Na_3PSO_3, MnO, $Na_3P(SO)_2$, Na_2MnS_2, $Na_4Mn_3S_5$, $Na_{1/3}MnS_2$, $Na_{2/3}MnS_2$, Na_3PO4	Na_2SO_4, Na_3PO_4, Na_3PS_4, $NaFeO_2$, Na_3PSO_3, Na_3PS_3O, FeS_2, Fe_3O_4, $Na_3P(SO)_2$, $Na_{3/2}FeS_2$	Na_2SO_4, Co, Na_3PO_4, Na_3PS_4, $NaCoO_2$, Co_9S_8, $NaCoS_2$, Na_2S, Na_3PSO_3, Na_3PS_3O, CoS_2, $Na_3P(SO)_2$, $Na_{2/3}CoS_2$, CoO	Na_2SO_4, $NaNiPO_4$, $Na_6S_2O_9$, Na_3PO_4, Ni_3S_4, Ni, Na_3PS_4, NaS, Na_2S, Na_3PSO_3, NaS_2, Ni_9S_8, Ni_3S_2, $Na_3P(SO)_2$, Na_3PS_3O, $Na_2Ni_3S_4$, NiO
Na_3PSe_4	$Na_2CrP_2O_7$, Cr_2O_3, Na_3PO_4, $Na_4P_2O_7$, Na_3PSe_4, Na_2SeO_3, $NaCrSe_2$, $Na_3Cr(PO_4)_2$, $NaCrO_2$, $NaSe_2$, NaSe, Na_3PSe_3O, Se	$MnSe_2$, Na_3PSe_4, Na_2MnSe_3, $NaMnO_2$, MnO, $NaSe_2$, Mn_3O_4, Na_2SeO_3, NaSe, $NaMnPO_4$, Na_3PO_4	Na_3PSe_4, $FeSe_2$, FeSe, Na_3PSe_3O, Na_3PO_4, $Na_4P_2O_7$, Fe_2O_3, FeO, Na_3PSeO_3, $NaSe_2$, Fe_2P, FeP, Na_2SeO_3, $NaFeO_2$, NaSe, Fe_3O_4, Na_2Se	Na_3PSe_4, Na_3PSe_3O, $CoSe_2$, $Na_4P_2O_7$, $NaCo_7O_{11}$, Na_3PSeO_3, Na_2SeO_3, Co_3O_4, Co_2P, Na_2Se, Co_5Se_8, CoO, Na_3PO_4	Na_3PSe_4, Ni_2P, Na_3PSe_3O, NiO, $Na_4P_2O_7$, Na_2SeO_4, Na_4SeO_5, Na_3PSeO_3, Na_2SeO_3, Ni_5Se_8, $NiSe_2$, NaSe, $Ni_{12}P_5$, Na_2Se, Na_3PO4

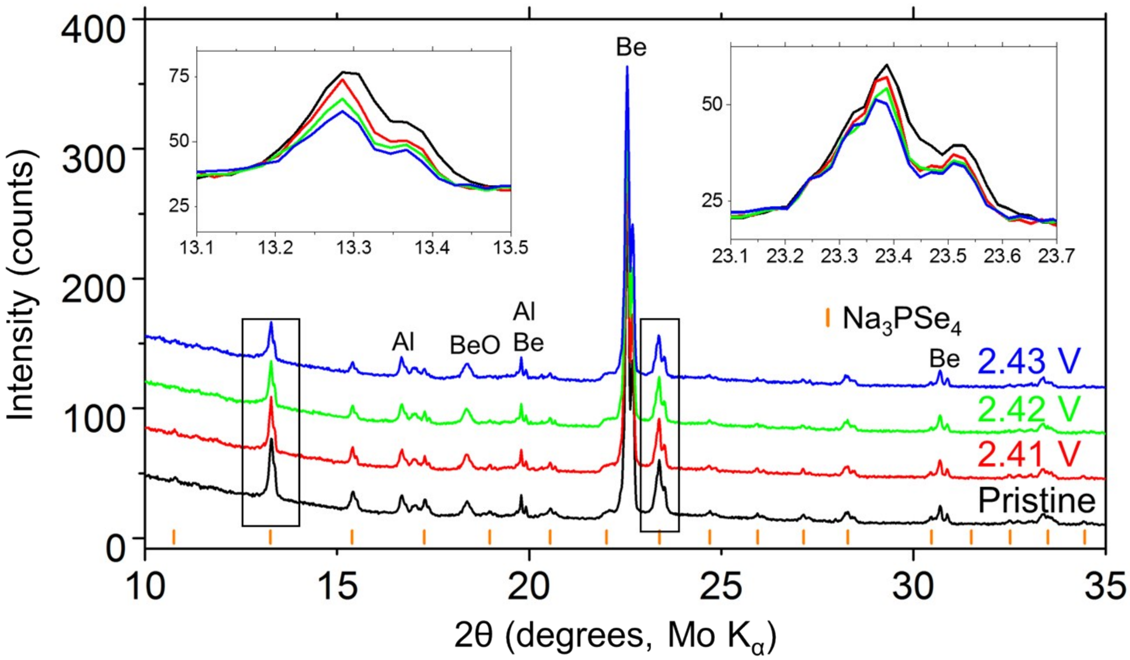

Fig. S1: *In situ* XRD patterns of Na_3PSe_4 cathode composite during the charging process. The insets show the intensity change, demonstrating the growth of Se at the expense of Na_3PSe_4.

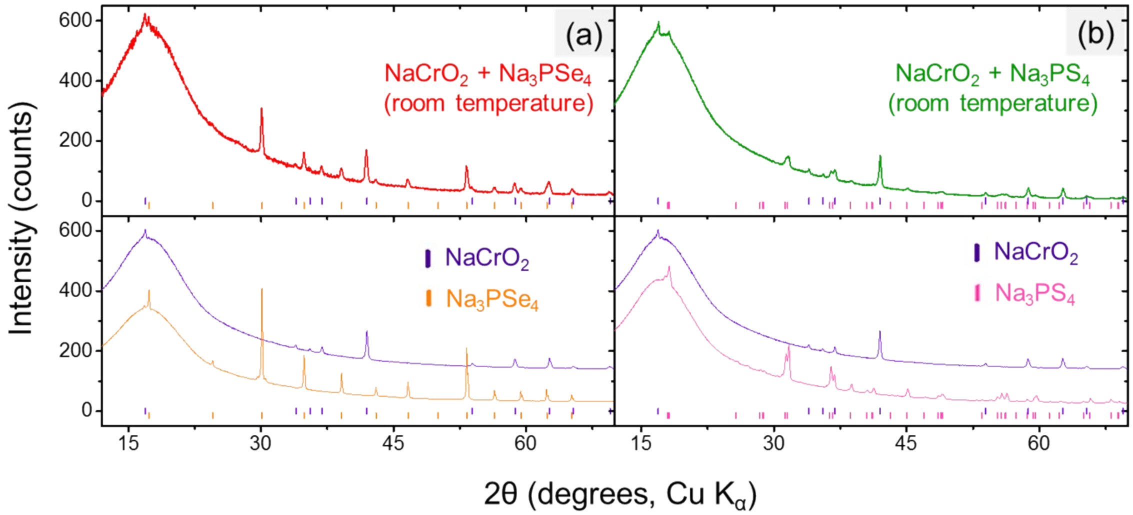

Fig. S2 (a–b) Diffraction patterns of $NaCrO_2$, Na_3PX_4, and mixture of the paired materials at RT (25°C); the tick marks indicate $NaCrO_2$ (purple, top) and Na_3PX_4 (orange for Na_3PSe_4, pink for Na_3PS_4, bottom) peaks. The diffraction pattern of the mixed materials is almost the same as the sum of those of each individual component, suggesting that no bulk reaction occurs between $NaCrO_2$ and Na_3PX_4 after mixing at RT.

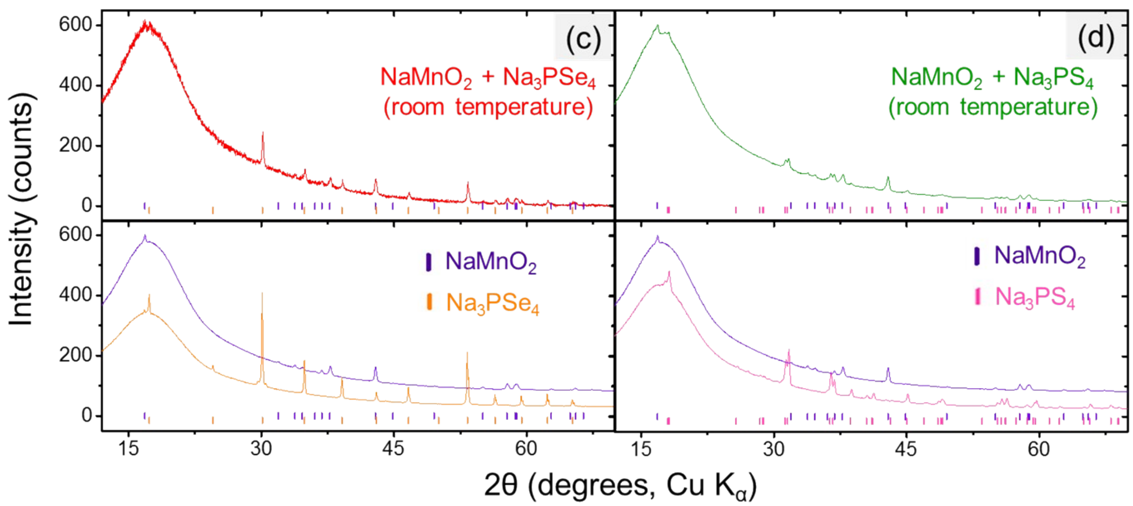

Fig. S2 (c–d) Diffraction patterns of $NaMnO_2$, Na_3PX_4, and a mixture of the paired materials at RT (25°C); the tick marks indicate $NaMnO_2$ (purple, top) and Na_3PX_4 (orange for Na_3PSe_4, pink for Na_3PS_4, bottom) peaks. No bulk reaction is observed between $NaMnO_2$ and Na_3PX_4 after mixing at RT.

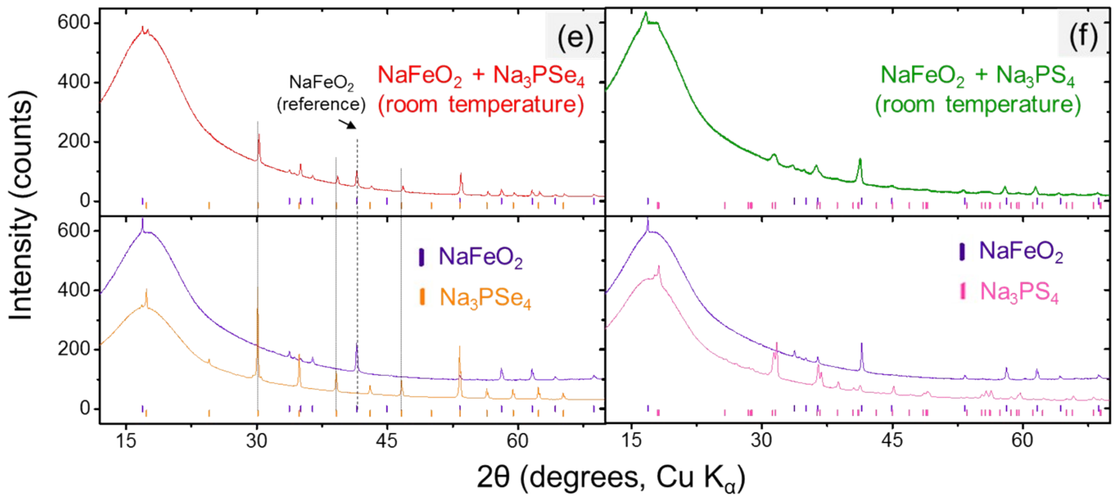

Fig. S2 (e–f) Diffraction patterns of $NaFeO_2$, Na_3PX_4, and a mixture of the paired materials RT (25°C); the tick marks indicate $NaFeO_2$ (purple, top) and Na_3PX_4 (orange for Na_3PSe_4, pink for Na_3PS_4, bottom) peaks. Peak shifts are observed in (e) at 30°, 39°, and 46°, indicating that $NaFeO_2$ reacts with Na_3PSe_4 at RT. Note that only peak shifts of Na_3PSe_4 are observed (one peak of $NaFeO_2$ is marked as reference). No bulk reaction is observed between $NaCrO_2$ and Na_3PS_4 after mixing at RT in (f).

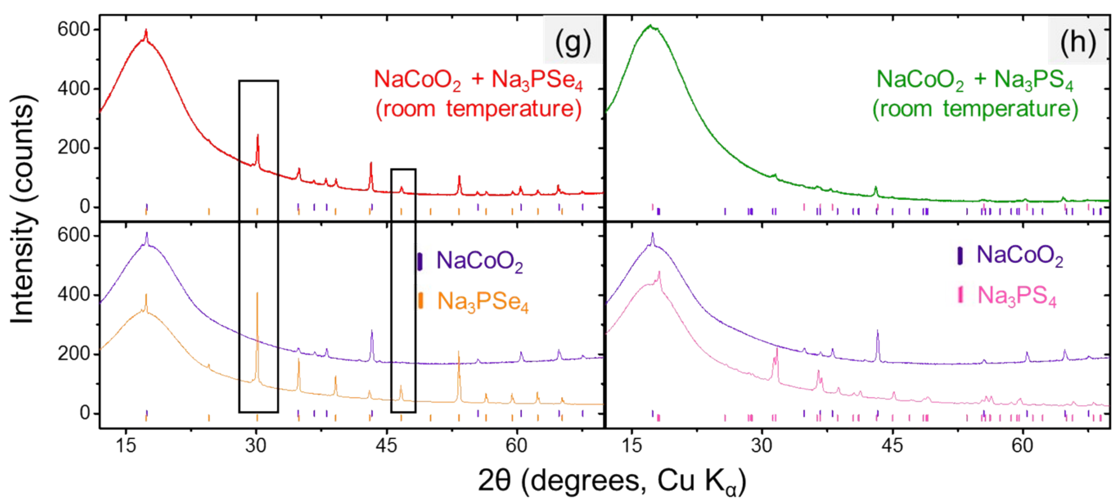

Fig. S2 (g–h) Diffraction patterns of $NaCoO_2$, Na_3PX_4, and a mixture of the paired materials at RT (25°C); the tick marks indicate $NaCoO_2$ (purple, top) and Na_3PX_4 (orange for Na_3PSe_4, pink for Na_3PS_4, bottom) peaks. Peak shape changes are observed in (g) at 30° and 46°, indicating that $NaCoO_2$ reacts with Na_3PSe_4 at RT. No bulk reaction is observed between $NaCoO_2$ and Na_3PS_4 after mixing at RT in (h).

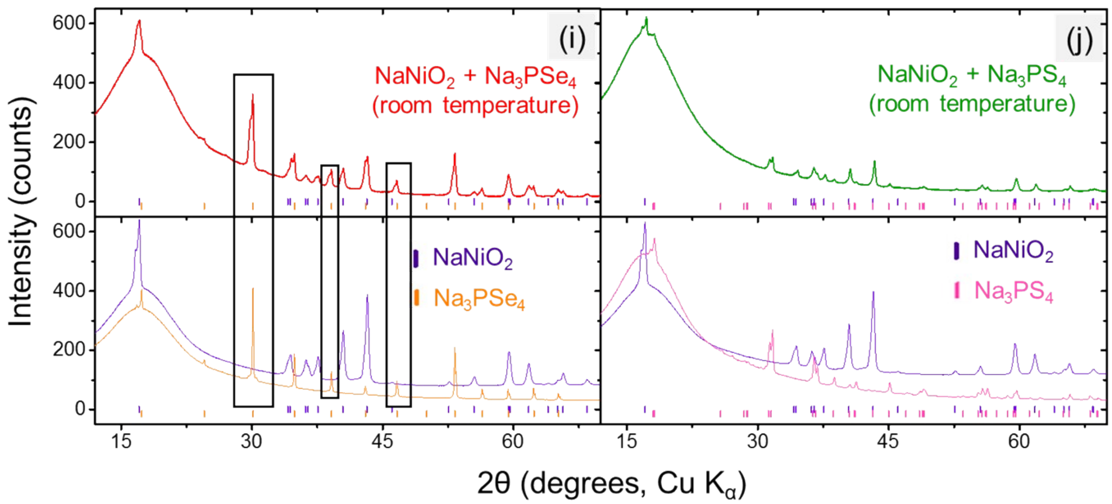

Fig. S2 (i–j) Diffraction patterns of $NaNiO_2$, Na_3PX_4, and a mixture of the paired materials at RT (25°C); the tick marks indicate $NaNiO_2$ (purple, top) and Na_3PX_4 (orange for Na_3PSe_4, pink for Na_3PS_4, bottom) peaks. Peak shape changes are observed in (i) at 30°, 39°, and 46°, indicating that $NaNiO_2$ reacts with Na_3PSe_4 at RT. No bulk reaction is observed between $NaNiO_2$ and Na_3PS_4 after mixing at RT in (j).

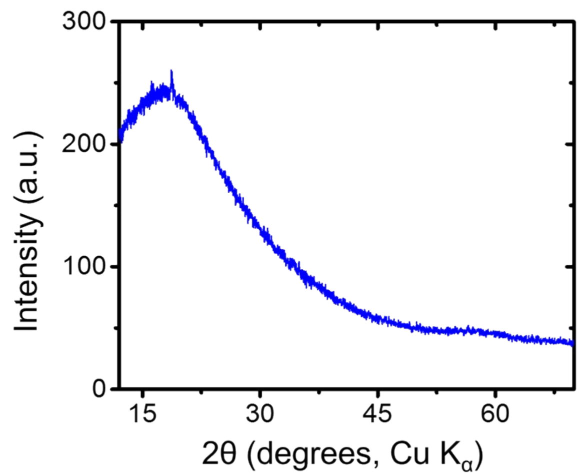

Fig. S3 Diffraction pattern of Kapton sample holder.

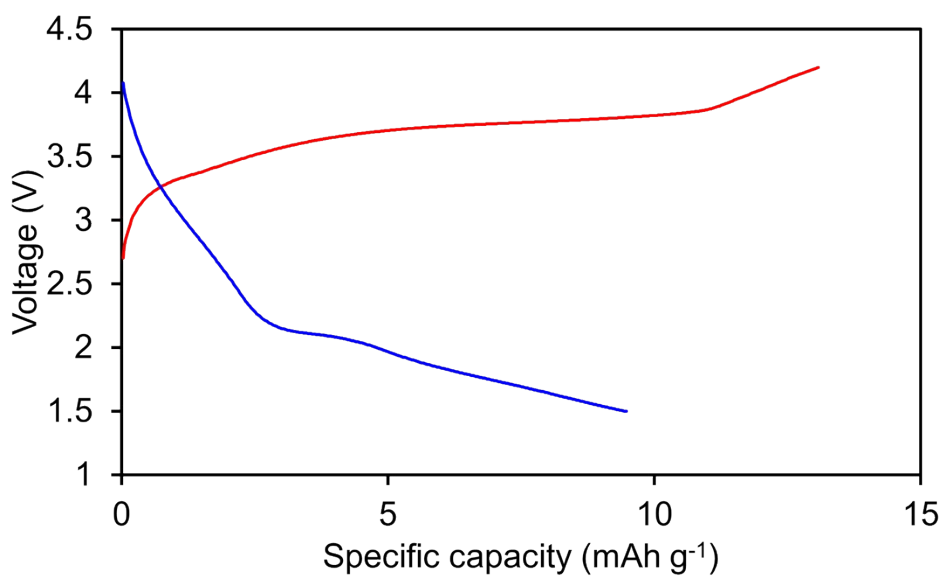

Fig. S4 Electrochemical measurement of β-$NaFeO_2$ (cut-off voltage: 4.0 V for charging, 1.5 V for discharging), demonstrating the electrochemical inactivity of β-$NaFeO_2$.

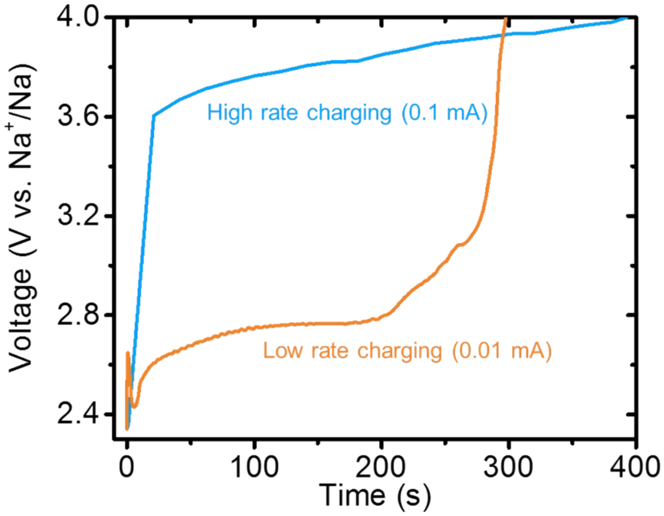

Fig. S5 Comparison of the charging process of Na_3PS_4 at high rate (0.1 mA) and low rate (0.01 mA).

Table S2: Synthesis conditions of Na$M$$O_2$ cathode materials

	Precursors	Heating Condition	Reference
$NaCrO_2$	Cr_2O_3 (Sigma–Aldrich, >99.5%), Na_2CO_3 (Sigma–Aldrich, 99%)	900°C in Ar (with 2% H_2) for 10 h	[39]
$NaMnO_2$	Mn_2O_3 (Sigma–Aldrich, >99.5%), Na_2CO_3 (Sigma–Aldrich, 99%)	700°C in air for 9 h	[40]
$NaFeO_2$	Fe_2O_3 (Sigma–Aldrich, >99%), Na_2O_2 (Sigma–Aldrich, 97%)	600°C in air for 20 h	[41]
$NaCoO_2$	Co_3O_4 (Sigma–Aldrich, 99.5%), Na_2O_2 (Sigma–Aldrich, 97%)	550°C in O_2 for 16 h	[42]
$NaNiO_2$	NiO (Sigma–Aldrich, 99%), Na_2O_2 (Sigma–Aldrich, 97%)	650°C in O_2 for 10 h	[43]

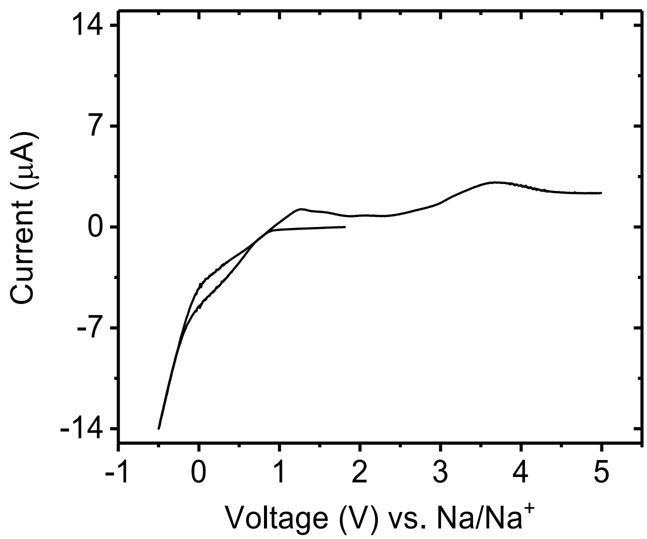

Fig. S6 Cyclic voltammogram of the Na_3PSe_4 solid-state electrolyte. A platinum foil, as the working electrode, and a sodium foil, as the counter/reference electrode, were used. The potential sweep was performed with a scanning rate of 5 mV s^{-1} at 25 °C.